pH Modulates Friction Memory Effects in Protein Folding

Benjamin A. Dalton and Roland R. Netz*
Freie Universität Berlin, Fachbereich Physik, 14195 Berlin, Germany

(Received 25 January 2024; accepted 24 September 2024; published 29 October 2024)

Protein folding is an intrinsically multitimescale problem. While it is accepted that non-Markovian effects are present on short timescales, it is unclear whether memory-dependent friction influences long-timescale protein folding reaction kinetics. We combine friction memory-kernel extraction techniques with recently published extensive all-atom simulations of the α3D protein under neutral and reduced pH conditions, and we show that the pH reduction modifies the friction acting on the folding protein by dramatically decreasing the friction memory decay time. This switches α3D folding reaction kinetics from the pronounced non-Markovian regime, where memory significantly accelerates folding, to the Markovian regime, where memory does not influence the folding time. We explore salt-bridge interactions, which are eliminated under pH reduction, as a key microscopic origin of non-Markovian friction in α3D.

DOI: 10.1103/PhysRevLett.133.188401

Molecular friction is essential for describing the folding dynamics of proteins. For example, the nonlinear dependence of protein folding rates on solvent viscosity has long been discussed in terms of internal friction effects [1–11], where intramolecular interactions within the protein are considered distinct from friction due to protein-solvent interactions. Despite its centrality in the theoretical description of protein folding, friction remains difficult to evaluate directly from experimental or detailed atomistic simulation data. Traditionally, it has been assumed that the folding rates are described by a particular reaction-kinetic model, allowing the friction to be determined by a fitting procedure [12,13]. This assumption dismisses alternative models that cannot be validated using the fitted friction coefficients. Markovian models have been successfully applied to model protein folding [14–16]. However, these models neglect the role of non-Markovian friction, implying that such effects occur rapidly compared to other relevant timescales, such as folding times. Two problems with this approach are that (i) it has been shown that non-Markovian effects can still influence barrier-crossing kinetics when memory timescales are short compared to barrier-crossing timescales [17], and (ii) proteins have been shown to exhibit long memory timescales that are comparable to the folding timescales [18]. While non-Markovian effects have been considered in protein folding [19,20], it is only recently that memory kernel extraction techniques [21–23], which enable the quantitative evaluation of time-dependent friction kernels on arbitrary reaction coordinates, have been applied to extensive protein folding simulation trajectories [18,24]. These techniques have been validated for a range of molecular systems [22,23,25–27] and have opened the way for the direct non-Markovian analysis of time series data generated by a wide range of complex systems. In this Letter, we combine non-Markovian memory kernel extraction techniques with recently published extensive molecular dynamics simulation data to isolate the first conclusive example of memory-dependent friction affecting protein folding rates.

α3D is a 73-residue, fast-folding designed protein [28,29] that folds into a tertiary structure comprising three interacting α-helical subunits [Fig. 1(a)], exhibiting distinct folded and unfolded states at neutral pH in both experiments [30] and simulations [31]. The folding kinetics of the α3D protein are strongly influenced by several native and non-native salt-bridge interactions between the positively charged side groups of lysine and arginine and the negatively charged side groups of aspartate and glutamate [32,33]. These salt bridges interact between residue-chain segments associated with the distinct helices, even when unfolded [33]. Recently, the folding kinetics of the α3D protein were compared under low and neutral pH conditions using both experiments and all-atom simulations [32]. It was shown that lowering the pH significantly reduces both native and non-native salt-bridge interactions, thereby reducing the stability of the folded state. The reduction in the stability of the folded state due to pH changes has been addressed in previous simulation studies for different proteins [34]. However, in the case of α3D, the pH reduction also increases the folding rate. In this Letter, we analyze all-atom simulation data for the α3D protein under low and neutral pH conditions (see Supplemental Material, Sec. I [35]), and we demonstrate that pH reduction significantly perturbs non-Markovian folding friction. Using memory kernel extraction techniques, we show that both the total friction and the non-Markovian memory timescale are significantly reduced when the pH is

*Contact author: rnetz@physik.fu-berlin.de

lowered, so much so that the non-Markovian features that dominate α3D folding kinetics at neutral pH are eliminated, thereby allowing for an accurate Markovian model description of the low pH folding kinetics. The same Markovian model fails to describe α3D folding in neutral pH conditions, underpredicting the folding rates by a factor of 6, indicating strong non-Markovian barrier-crossing acceleration effects at neutral pH.

To track the folding progress of the α3D protein, we project the atomic coordinates onto the fraction of native contacts reaction coordinate, Q [33,40] [Fig. 1(b) and Supplemental Material, Sec. II [35]]. Q has been shown to optimally reveal the transition state for a range of proteins [33], including the neutral α3D protein studied here and, thus, is a good reaction coordinate according to the transition-state ensemble method [39,41,42]. For our analysis, it is important to demonstrate that Q is an equally good reaction coordinate for α3D under both pH conditions in the following sense. In both cases, Q exhibits distinct two-state distributions [Fig. 1(c) and Supplemental Material, Fig. S1(c) [35]] and a sharply peaked conditional transition-path probability $P(TP|Q) = P(Q|TP)P(TP)/P(Q)$, i.e., the probability to be on a transition path when at Q [39] [Fig. 1(c) inset and Supplemental Material, Sec. II [35]]. $P(Q)$ and $P(TP)$ are the probability density function of Q and the probability to be on a transition path, respectively. $P(Q|TP)$ is the probability density conditional to being on a transition path. $P(TP|Q)$ provides a measure of the quality of a reaction coordinate, such that a sharply peaked value of 0.5, which is approximately the case for both α3D systems, indicates a transition state in 1D Markovian theory. These results suggest that non-Markovian effects should be negligible [20], which we later demonstrate is incorrect.

Because of the strong asymmetry in the free-energy profiles [Fig. 1(c)] and the large differences between the folded-state energies, we consider transitions that connect the unfolded state minimum Q_u to the barrier top Q_b. We define the folding times τ^{MD}_{MFP} in the MD simulations as the mean first-passage (MFP) times from Q_u to Q_b. Using this method, the folding times are evaluated as $\tau^{MD}_{MFP} = 5.2$ μs and $\tau^{MD}_{MFP} = 6.4$ μs for the low and neutral pH systems, respectively. Previous analysis of the same data reported average residence times of 10 μs for low pH and 20 μs for neutral pH [32], where a residence time is defined as the duration spent in the unfolded state before traversing the barrier to reach the folded state minimum, Q_f. These results are compared to experimental folding times of approximately 6 μs for low pH [29] and 10 μs for neutral pH [30]. Residence times and mean first-passage times are known to diverge for non-Markovian systems due to recrossing effects [43]. In Supplemental Material Sec. III [35], we discuss the different definitions of folding times, the role of recrossing, and present various folding time distributions and error estimates. Regardless of the definition used, the low pH system folds faster than the neutral system. This

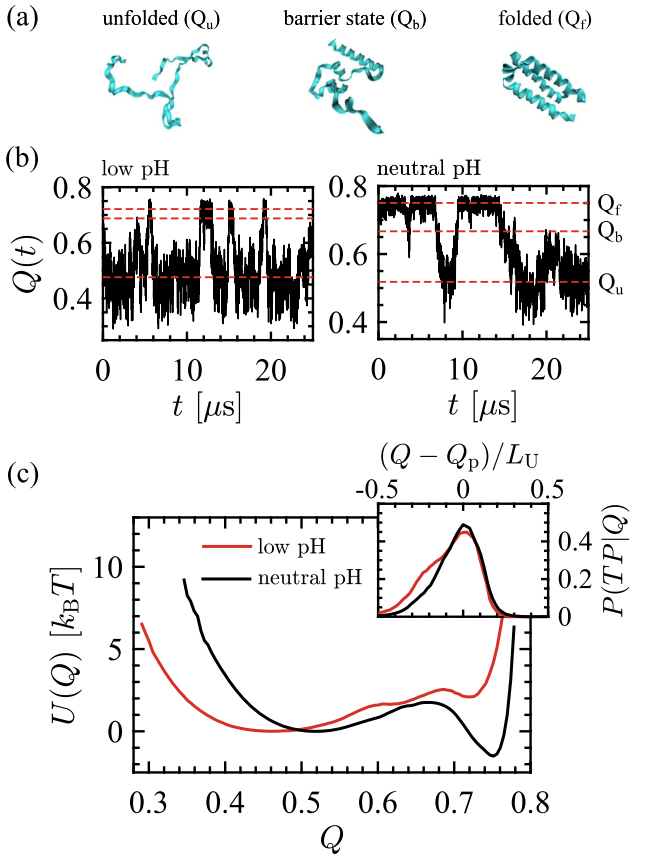

FIG. 1. Folding dynamics of the α3D protein. (a) Simulation snapshots of representative states for neutral pH. All-atom trajectories taken from [31,32]. (b) 25 μs trajectory segments for the fraction of native contacts Q reaction coordinate for α3D for low pH = 2 and neutral pH = 7. The unfolded, barrier top, and folded states are indicated by Q_u, Q_b, and Q_f, respectively (red dashed lines). (c) Fraction of native contacts free-energy profiles $U(Q) = -k_BT \log[P(Q)]$ for the two pH conditions. $P(Q)$ is the Q probability density. Inset: conditional probabilities to be on a transition path $P(TP|Q)$ at position Q, suggesting that Q is a good reaction coordinate for the all-atom α3D trajectories under both pH conditions [39]. For comparison, Q is shifted by the peak value Q_p, often identified as the transition state, and rescaled by the distance between free-energy minima $L_U = Q_f - Q_u$.

difference cannot be explained by stability changes since, as previously noted [32], the folding barrier is slightly higher for the low pH system [$\Delta U = 1.7k_BT$ for neutral pH and $\Delta U = 2.6k_BT$ for low pH, Fig. 1(c)]. Thus, the reduced folding time for low pH must result from friction effects.

To evaluate the friction, we map the $Q(t)$ trajectories for α3D onto a generalized Langevin equation [44–47], as given by

$$m\ddot{Q}(t) = -\int_0^t \Gamma(t-t')\dot{Q}(t')dt' - \nabla U[Q(t)] + \xi(t). \quad (1)$$

$\Gamma(t)$ is the friction memory kernel, $U(Q)$ is the free-energy profile [Fig. 1(c)], and m is the effective mass of Q, which

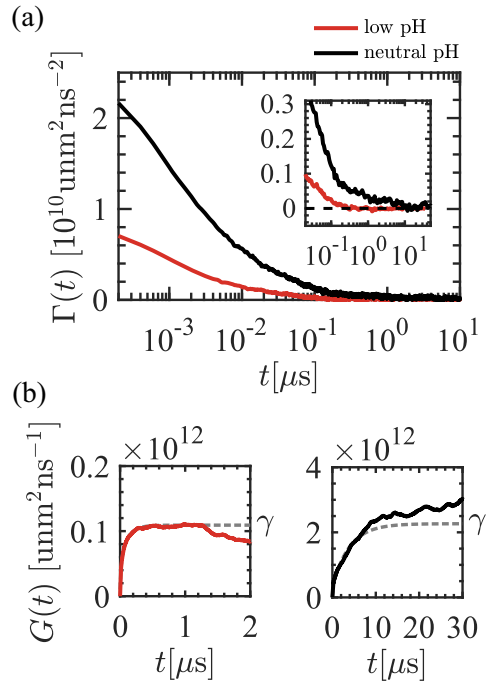

FIG. 2. Friction and memory effects in α3D dynamics. (a) Memory kernels $\Gamma(t)$, extracted for two different pH conditions. Inset: a magnification of the long-time behavior. (b) Running integrals $G(t)$ for the two memory kernels extracted in (a) (bold lines). The dashed lines represent running integrals derived from four-component exponential fits of the memory kernel data in (a) (see Supplemental Material, Sec. IV, for details on fitting [35]). The total friction γ is determined by the plateau value of $G(t \to \infty)$, obtained from the fitted curves.

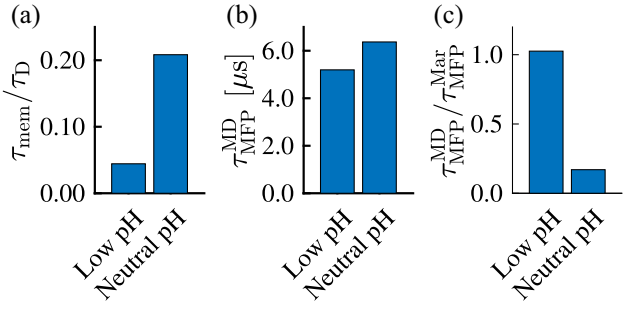

FIG. 3. Comparison of the dynamic timescales for α3D folding under two pH conditions. (a) The ratio of the memory time τ_{mem} and diffusion time τ_D indicates more pronounced non-Markovian effects at neutral pH. (b) Mean first-passage times from MD simulations for transitions from unfolded state minimum to barrier top. (c) Comparison of mean first-passage times τ^{MD}_{MFP}, from reactant state Q_u to target state Q_b, measured in simulations and a purely Markovian prediction τ^{Mar}_{MFP} [Eq. (2)]. At low pH, the Markovian model accurately predicts τ^{MD}_{MFP}. At neutral pH, the MD simulation transition time is significantly faster than the Markovian prediction, indicating non-Markovian acceleration effects.

is assumed to have no position dependence [18]. $\xi(t)$ is the random force term approximately satisfying the fluctuation-dissipation theorem $\langle \xi(t)\xi(t')\rangle = k_B T \Gamma(t-t')$, where $k_B T$ is the thermal energy. Using recent memory kernel extraction techniques, we directly extract the running integral of the memory kernel $G(t) = \int_0^t \Gamma(t')dt'$ from the time series of $Q(t)$ [23,24], where the total friction γ acting on $Q(t)$ is determined by the plateau value $\gamma = G(t \to \infty)$. In Fig. 2(a), we show the memory kernels for the α3D protein under the two pH conditions (for additional information, see Supplemental Material, Sec. IV [35]). Lowering the pH in the MD simulations decreases both the amplitude and the decay time of the memory. The latter is evident in the long-time tails, as magnified in the inset. The memory kernel for neutral pH spans microseconds, while for low pH, the decay is over an order of magnitude faster. From the running integrals $G(t)$ in Fig. 2(b), we see that the total friction γ is reduced by a factor of $\sim$23. Thus, while the amplitude of $\Gamma(t)$ is reduced by a factor of $\sim$2 at short times, the dramatic reduction in total friction is primarily due to the reduced friction memory time.

We evaluate the memory decay time via the first moment of the memory kernel, $\tau_{mem} = \int_0^\infty t\Gamma(t)dt / \int_0^\infty \Gamma(t)dt$, obtaining $\tau_{mem} = 3.4$ μs and 0.07 μs for the neutral and low pH systems, respectively. After extracting the friction coefficient, we can evaluate other characteristic timescales associated with folding dynamics. The diffusion time $\tau_D = \gamma(Q_b - Q_u)^2/k_B T$ is the time to diffuse from the unfolded state to the barrier top in the absence of a free-energy profile (a table of all relevant timescales and extracted system parameters is provided in Supplemental Material, Sec. I [35]). Memory effects are expected to influence barrier-crossing kinetics when $1 \times 10^{-2} < \tau_{mem}/\tau_D < 1 \times 10^1$ [17]. While this condition is well satisfied for the neutral pH system, it is only marginally met for the low pH system [Fig. 3(a)]. Therefore, we expect non-Markovian effects to be more pronounced for the neutral pH system.

In Fig. 3(b), we show the folding mean first-passage times for the two pH conditions from MD simulations. To quantify deviations from Markovianity, we predict transition times using the following Markovian overdamped formula, which exactly accounts for the free-energy profiles shown in Fig. 1(c) [48]:

$$\tau^{Mar}_{MFP} = \frac{\gamma}{k_B T}\int_{Q_u}^{Q_b} dx e^{U(x)/k_B T}\int_{-\infty}^{x} dy e^{-U(y)/k_B T}. \quad (2)$$

The application of Eq. (2) for purely Markovian systems on arbitrary free-energy landscapes is discussed in Supplemental Material, Sec. V [35]. Deviations between τ^{Mar}_{MFP} and τ^{MD}_{MFP} can be due to either the neglect of position-dependent friction or the presence of memory effects. Recent studies show that a position-dependent Markovian friction cannot consistently describe both the folding and unfolding processes [18,24], suggesting this model is unsuitable for protein folding (this analysis pertains to the

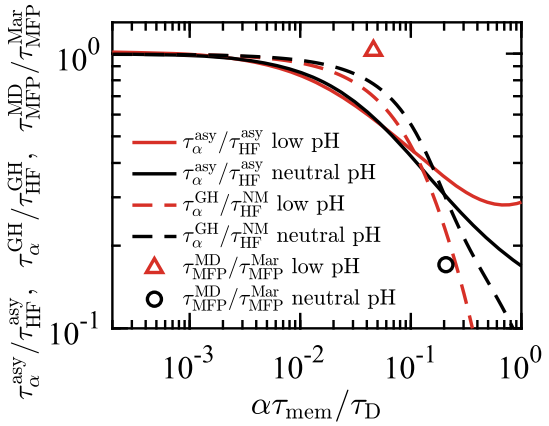

FIG. 4. Predictions for non-Markovian barrier crossing over a range of memory timescales are made using an asymptotic cross-over formula, $\tau_\alpha^{\rm asy}/\tau_{\rm HF}^{\rm asy}$ (solid lines), and the Grote-Hynes theory, $\tau_\alpha^{\rm GH}/\tau_{\rm HF}^{\rm GH}$ (dashed lines), parametrized by a four-component exponential fit for the memory kernels in Fig. 2(a). All memory times are scaled by a common factor, α, and each prediction is normalized to its respective high-friction (HF) Markovian limit ($\tau_{\rm HF}^{\rm asy}$ and $\tau_{\rm HF}^{\rm GH}$). Colored symbols represent $\tau_{\rm MD}^{\rm MFP}/\tau_{\rm Mar}^{\rm MFP}$, located at $\alpha\tau_{\rm mem}$ for $\alpha = 1$.

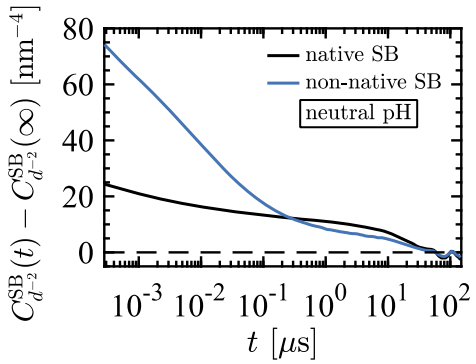

FIG. 5. The autocorrelation function of the inverse square of the separation distance between salt bridges (SB) is calculated from lists of all native (black) and non-native (blue) salt-bridge pairs. At neutral pH, this correlation function serves as a proxy for time-dependent salt-bridge friction. Such friction does not exist at low pH, where salt bridges are eliminated.

neutral α3D protein discussed here [18]). Comparing $\tau_{\rm MFP}^{\rm Mar}$ and $\tau_{\rm MFP}^{\rm MD}$ for the two pH systems shows that Eq. (2) predicts the transition time for the low pH system [Fig. 3(c)]. This is expected since the memory timescale approaches $1 \times 10^{-2}\tau_{\rm D}$, so α3D exhibits effectively Markovian folding, consistent with a model having position-independent, memoryless friction. However, folding in the neutral pH system is accelerated sixfold compared to the Markovian prediction [Fig. 3(c)].

Barrier-crossing acceleration is a hallmark of non-Markovian reactive processes and is predicted by various non-Markovian reaction-rate theories. In Fig. 4, we compare the simulation results with two different non-Markovian predictions, confirming that the neutral-pH system folds rapidly, despite significantly higher total friction, due to memory speedup effects. We parametrized both the Grote-Hynes (GH) theory [49] and a recent asymptotic cross-over formula [17,50,51] by fitting the memory kernels to $\Gamma(t) = \sum_{n=1}^{4} \gamma_n e^{-t/\tau_n}/\tau_n$ (Supplemental Material, Sec. VI [35]) and uniformly scaling all memory times τ_n that enter each prediction by a common factor α. $\tau_\alpha^{\rm asy}/\tau_{\rm HF}^{\rm asy}$ is the asymptotic cross-over formula [50,51], rescaled by the high-friction (overdamped) Markovian limit $\tau_{\rm HF}^{\rm asy}$ (Supplemental Material, Sec. VI [35]). $\tau_\alpha^{\rm asy}$ was recently shown to be accurate for predicting the folding and unfolding times of a large population of fast-folding proteins [18], even capturing the non-Markovian barrier-crossing slow-down regime in some instances. Similarly, $\tau_\alpha^{\rm GH}/\tau_{\rm HF}^{\rm GH}$ is the rescaled Grote-Hynes prediction (Supplemental Material, Sec. VI [35]). In Fig. 4, we show both predictions, plotted as a function of the first-moment memory time associated with the α scaling ($\alpha\tau_{\rm mem}$). Both models predict reaction acceleration when $\tau_{\rm mem}/\tau_{\rm D} > 1 \times 10^{-2}$. When considering the values for $\tau_{\rm MD}^{\rm MFP}/\tau_{\rm Mar}^{\rm MFP}$ given in Fig. 3(c) (replotted in Fig. 4), we see that the deviations from Markovianity in the neutral-pH system are expected since it is deep in the memory-induced speedup regime predicted by both non-Markovian models. Likewise, the low pH system aligns well with the Markovian limit; deviations are likely because both non-Markovian models incorporate harmonic approximations to the free-energy profiles, which are not well represented for the two α3D systems.

It is desirable to understand the molecular origins of non-Markovian friction. We utilize physicochemical perturbation through pH reduction to reveal the key role of native and non-native salt-bridge interactions, previously shown to dominate the folding transition paths in α3D [32,33]. In Fig. 5, we show autocorrelation functions for the inverse square of the separation distance $C_{d^{-2}}^{\rm SB}(t) = \sum_{i,j}\langle d_{ij}^{-2}(t) d_{ij}^{-2}(0)\rangle$, where i and j are the indices for the charged atoms with positions $\mathbf{r}_i$ and $\mathbf{r}_j$, calculated uniquely for the sets of native and non-native salt-bridge pairs (see Supplemental Material, Sec. VII, for details [35]). $d_{i,j} = |\mathbf{r}_i - \mathbf{r}_j|$ is the separation distance between charges and $d_{ij}^{-2}(t)$ is proportional to the Coulomb force associated with a given salt bridge and, therefore, $C_{d^{-2}}^{\rm SB}(t) - C_{d^{-2}}^{\rm SB}(\infty)$ serves as a proxy for the time-dependent friction due to salt-bridge Coulomb interactions [52]. Subtracting $C_{d^{-2}}^{\rm SB}(\infty)$ ensures the decay to zero for long times and thus accounts for other force contributions to the friction. The correlations in Fig. 5 show that both the native and non-native salt-bridge populations exhibit correlation timescales similar in magnitude to the memory kernels of $Q(t)$ for the neutral pH α3D in Fig. 2(a). In Fig. S7 of the Supplemental Material, Sec. VII [35], we show that correlations between the same atomic pairs at low pH, where the Coulomb force between atomic pairs is eliminated, resulting in the

elimination of salt-bridge friction, have significantly reduced correlation timescales. This suggests salt bridges as the molecular origin of the different friction memory effects at high and low pH. Overall, understanding molecular origins of non-Markovian friction is a important direction for future research.

Finally, we mention that the transition from non-Markovian to Markovian reaction kinetics under pH reduction is consistent when measured in alternative reaction coordinates, as long as the coordinate reflects the protein's barrier-separated two-state behavior (see Supplemental Material, Sec. VIII [35]). For reaction coordinates that do not exhibit distinct transition states, such as the radius of gyration (see Supplemental Material, Fig. S8 [35]), it is still possible to observe a significant pH-sensitive reduction in friction memory times, as we observe with the memory kernels extracted from the Q trajectories. However, the quality of these reaction coordinates cannot be assessed using transition-state ensemble methods [39,41,42] and standard barrier-crossing kinetic models do no apply.

Acknowledgments—We acknowledge support by the ERC Advanced Grant No. 835117 MaMemo and by the DFG vis SFB 1078 project ID 221545957. We thank D. E. Shaw Research for providing the all-atom simulation data that we analyze in this Letter.

[1] D. Beece, L. Eisenstein, H. Frauenfelder, D. Good, M. C. Marden, L. Reinisch, A. H. Reynolds, L. B. Sorensen, and K. T. Yue, Biochemistry **19**, 5147 (1980).
[2] W. Doster, Biophys. Chem. **17**, 97 (1983).
[3] A. Ansari, C. M. Jones, E. R. Henry, J. Hofrichter, and W. A. Eaton, Science **256**, 1796 (1992).
[4] G. S. Jas, W. A. Eaton, and J. Hofrichter, J. Phys. Chem. B **105**, 261 (2001).
[5] S. J. Hagen, Curr. Protein Pept. Sci. **11**, 385 (2010).
[6] A. Soranno, B. Buchli, D. Nettels, R. R. Cheng, S. Müller-Späth, S. H. Pfeil, A. Hoffmann, E. A. Lipman, D. E. Makarov, and B. Schuler, Proc. Natl. Acad. Sci. U.S.A. **109**, 17800 LP (2012).
[7] A. Borgia, B. G. Wensley, A. Soranno, D. Nettels, M. B. Borgia, A. Hoffmann, S. H. Pfeil, E. A. Lipman, J. Clarke, and B. Schuler, Nat. Commun. **3**, 1195 (2012).
[8] J. C. F. Schulz, L. Schmidt, R. B. Best, J. Dzubiella, and R. R. Netz, J. Am. Chem. Soc. **134**, 6273 (2012).
[9] I. Echeverria, D. E. Makarov, and G. A. Papoian, J. Am. Chem. Soc. **136**, 8708 (2014).
[10] D. de Sancho, A. Sirur, and R. B. Best, Nat. Commun. **5**, 4307 (2014).
[11] W. Zheng, D. De Sancho, T. Hoppe, and R. B. Best, J. Am. Chem. Soc. **137**, 3283 (2015).
[12] G. Hummer, New J. Phys. **7**, 34 (2005).
[13] I. V. Gopich and A. Szabo, J. Phys. Chem. B **113**, 10965 (2009).
[14] V. Muñoz and W. A. Eaton, Proc. Natl. Acad. Sci. U.S.A. **96**, 11311 (1999).
[15] R. B. Best and G. Hummer, Phys. Rev. Lett. **96**, 228104 (2006).
[16] W. Zheng and R. B. Best, J. Phys. Chem. B **119**, 15247 (2015).
[17] J. Kappler, J. O. Daldrop, F. N. Brünig, M. D. Boehle, and R. R. Netz, J. Chem. Phys. **148**, 14903 (2018).
[18] B. A. Dalton, C. Ayaz, H. Kiefer, A. Klimek, L. Tepper, and R. R. Netz, Proc. Natl. Acad. Sci. U.S.A. **120**, e2220068120 (2023).
[19] S. S. Plotkin and P. G. Wolynes, Phys. Rev. Lett. **80**, 5015 (1998).
[20] A. M. Berezhkovskii and D. E. Makarov, J. Phys. Chem. Lett. **9**, 2190 (2018).
[21] B. J. Berne and G. D. Harp, Adv. Chem. Phys. **17**, 63 (1970).
[22] J. O. Daldrop, J. Kappler, F. N. Brünig, and R. R. Netz, Proc. Natl. Acad. Sci. U.S.A. **115**, 5169 (2018).
[23] B. Kowalik, J. O. Daldrop, J. Kappler, J. C. F. Schulz, A. Schlaich, and R. R. Netz, Phys. Rev. E **100**, 012126 (2019).
[24] C. Ayaz, L. Tepper, F. N. Brünig, J. Kappler, J. O. Daldrop, and R. R. Netz, Proc. Natl. Acad. Sci. U.S.A. **118**, e2023856118 (2021).
[25] F. N. Brünig, O. Geburtig, A. von Canal, J. Kappler, and R. R. Netz, J. Phys. Chem. B **126**, 1579 (2022).
[26] F. N. Brünig, J. O. Daldrop, and R. R. Netz, J. Phys. Chem. B **126**, 10295 (2022).
[27] B. A. Dalton, H. Kiefer, and R. R. Netz, Nat. Commun. **15**, 3761 (2024).
[28] S. T. R. Walsh, H. Cheng, J. W. Bryson, H. Roder, and W. F. DeGrado, Proc. Natl. Acad. Sci. U.S.A. **96**, 5486 (1999).
[29] Y. Zhu, D. O. V. Alonso, K. Maki, C.-Y. Huang, S. J. Lahr, V. Daggett, H. Roder, W. F. DeGrado, and F. Gai, Proc. Natl. Acad. Sci. U.S.A. **100**, 15486 (2003).
[30] H. S. Chung, I. V. Gopich, K. McHale, T. Cellmer, J. M. Louis, and W. A. Eaton, J. Phys. Chem. A **115**, 3642 (2011).
[31] K. Lindorff-Larsen, S. Piana, R. O. Dror, and D. E. Shaw, Science **334**, 517 (2011).
[32] H. S. Chung, S. Piana-Agostinetti, D. E. Shaw, and W. A. Eaton, Science **349**, 1504 (2015).
[33] R. B. Best, G. Hummer, and W. A. Eaton, Proc. Natl. Acad. Sci. U.S.A. **110**, 17874 (2013).
[34] E. P. O'Brien, B. R. Brooks, and D. Thirumalai, J. Am. Chem. Soc. **134**, 979 (2012).
[35] See Supplemental Material at http://link.aps.org/supplemental/10.1103/PhysRevLett.133.188401, which includes Refs. [36–38], for simulation details, additional details and discussion of reaction coordinates, and other additional analytical details.
[36] S. Piana, K. Lindorff-Larsen, and D. E. Shaw, Biophys. J. **100**, L47 (2011).
[37] L. Tepper, B. Dalton, and R. R. Netz, J. Chem. Theory Comput. **20**, 3061 (2024).
[38] X. Daura, K. Gademann, B. Jaun, D. Seebach, W. F. van Gunsteren, and A. E. Mark, Angew. Chem., Int. Ed. **38**, 236 (1999).
[39] G. Hummer, J. Chem. Phys. **120**, 516 (2004).
[40] E. Shakhnovich, G. Farztdinov, A. M. Gutin, and M. Karplus, Phys. Rev. Lett. **67**, 1665 (1991).

[41] P. L. Geissler, C. Dellago, and D. Chandler, J. Phys. Chem. B **103**, 3706 (1999).
[42] P. G. Bolhuis, D. Chandler, C. Dellago, and P. L. Geissler, Annu. Rev. Phys. Chem. **53**, 291 (2002).
[43] Q. Zhou, R. R. Netz, and B. A. Dalton, arXiv:2403.06604.
[44] R. Zwanzig, Phys. Rev. **124**, 983 (1961).
[45] H. Mori, Prog. Theor. Phys. **33**, 423 (1965).
[46] C. Ayaz, L. Scalfi, B. A. Dalton, and R. R. Netz, Phys. Rev. E **105**, 054138 (2022).
[47] H. Vroylandt, Europhys. Lett. **140**, 62003 (2022).
[48] R. Zwanzig, *Nonequilibrium Statistical Mechanics* (Oxford University Press, New York, 2001).
[49] R. F. Grote and J. T. Hynes, J. Chem. Phys. **73**, 2715 (1980).
[50] J. Kappler, V. B. Hinrichsen, and R. R. Netz, Eur. Phys. J. E **42**, 119 (2019).
[51] L. Lavacchi, J. Kappler, and R. R. Netz, Europhys. Lett. **131** (2020).
[52] K. Falk, F. Sedlmeier, L. Joly, R. R. Netz, and L. Bocquet, Nano Lett. **10**, 4067 (2010).